Available online at www.sciencedirect.com
ScienceDirect
Journal of Power Sources 160 (2006) 1017–1025
JOURNAL OF POWER SOURCES
www.elsevier.com/locate/jpowsour

Gas-phase particle image velocimetry (PIV) for application to the design of fuel cell reactant flow channels

S.Y. Yoon [a], J.W. Ross [b], M.M. Mench [b], K.V. Sharp [b,*]

[a] *201 RIMT, School of Mechanical Engineering, Pusan National University, Busan 609-735, Korea*
[b] *Microscale Flow Laboratory, Department of Mechanical and Nuclear Engineering, The Pennsylvania State University, 157D Hammond Building, University Park, PA 16802, USA*

Received 30 December 2005; received in revised form 9 February 2006; accepted 10 February 2006
Available online 29 March 2006

Abstract

Because the parasitic load on most polymer electrolyte fuel cell systems is dominated by pressure losses across the flow fields, understanding the flow channel dynamics has garnered significant recent attention. The current work is aimed at enabling advanced design of reactant flow channels by elucidating the details of the velocity fields within various reactant flow channel geometries. Gas-phase measurement is critical to ensuring that the results are valid for real fuel cell systems, and for application of this technique to the study of flow channels with two-phase obstruction phenomena. In the current research, gas-phase velocity fields have been measured using particle image velocimetry (PIV) in representative geometries, including a straight channel (for technique validation) and a 180° switchback with channel-to-land ratio of 1:1. The accuracy of the measurement depends on the ability of the seed particles to follow the flow. Numerical simulations have been performed to develop a criterion for identifying appropriate seed particles. The research presented is a first step toward measuring velocity fields in novel flow reactant channels in operational cells.

Keywords: Particle image velocimetry; PIV; Flow channel; Fuel cell; Velocity measurement; PEFC

1. Introduction

Recognizing that an operational polymer electrolyte fuel cell (PEFC) is an extremely complex system, advances in certain focused areas such as mass transport have the potential to contribute to improved performance of such systems. In an operational cell, reactant flow channels feed the gas over the electrode in any number of configurations, including parallel channels, serpentine channels, and parallel/serpentine combinations, among others [1]. In PEFCs, the formation of liquid droplets or films within the flow channel can drastically increase the already high parasitic load of the reactant flow on the overall system [2]. The measurement of the gas-phase velocity in these channels is expected to enable design of novel channel configurations with reduced parasitic load, particularly if velocity field measurements can be coupled with measurements of droplet or film dynamics on the surface of the gas diffusion media.

One geometry commonly encountered in actual cells is the 180° switchback. Martin et al. [3] measured and reported on the flow structures in a 180° switchback with characteristic dimension of approximately 10 mm and Reynolds numbers ranging from approximately 100–900. While Martin et al. [3] were interested in the flow of gas in a channel with 0.8 mm width, they actually measured the velocity in a liquid flow in a channel with characteristic dimension of approximately 10 mm. Based on the principle of Reynolds number similarity, the dynamics of a liquid flow and gas flow with the same Reynolds number should be equivalent. Fluid mechanicians commonly employ similarity principles to study flows that are not conducive to direct measurement, and the data from Martin et al. [3] serve as an excellent baseline for U-shaped reactant flow channel studies. However, in operational cells, two-phase flow phenomena may be present [2,4–9] and the development of a technique that can directly measure the gas-phase velocity in situ is important. To the authors' knowledge, Ladewig et al. [10] is the only study thus far that presents gas-phase data in an operational cell, and these measurements are yet preliminary. Ladewig et al.'s [10] strategy was to use laser Doppler anemometry (LDA) to measure

* Corresponding author. Tel.: +1 814 865 4292; fax: +1 814 863 7222.
E-mail address: kvs10@psu.edu (K.V. Sharp).

0378-7753/$ – see front matter © 2006 Elsevier B.V. All rights reserved.
doi:10.1016/j.jpowsour.2006.02.043

Nomenclature

C_c	slip correction factor
d_p	seed particle diameter
L	characteristic lengthscale
L_e	entrance length
L_x	cross-stream lengthscale
Re	Reynolds number ($=\rho UL\,\mu^{-1}$)
St	Stokes number
t	time
U	characteristic velocity scale
U_{max}	maximum velocity in channel
μ	viscosity
ρ	density
ρ_p	particle density

gas flow velocities in a U-shaped fuel cell channel with 2 mm × 2 mm cross section. The flow was seeded with water droplets, but the velocity data obtained were not yet complete enough to fully characterize the flow. Furthermore, LDA is a point-measurement technique while PIV, used in this study, is a field-measurement technique and as such can serve as more of a quantitative flow visualization technique than LDA.

The present study aims to develop a measurement technique that may be used in the future to *directly* measure gas-phase velocities in situ in an operational fuel cell. To that end, we use PIV to measure the gas-phase velocities in channels with characteristic dimensions of 1–2 mm. For PIV measurements in macro-scale gas flows, the gas is often seeded with olive oil particles generated by an atomizer. High pressure and a high flow rate are needed for the generation of the oil seed particles, but the flow in a fuel cell has a relatively low flow rate (Reynolds numbers of the order of hundreds to a few thousand). In the present study, representative measurements are

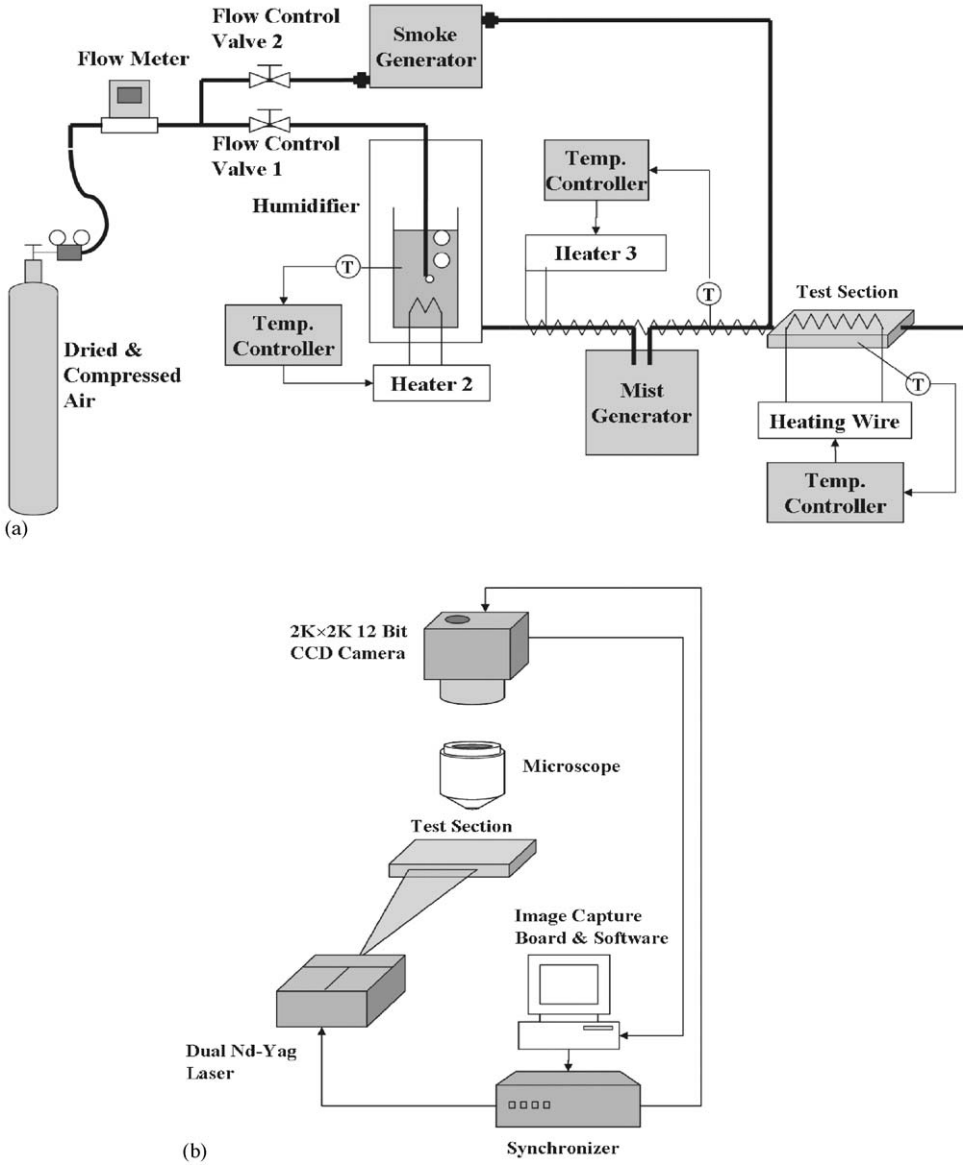

Fig. 1. (a) Flow delivery and temperature-control system setup. (b) Particle image velocimetry system setup.

made in millimeter-scale channels using two types of seed particles, namely smoke particles and water droplets. Seeding with water droplets is preferred since these may be introduced into humidified gas flows in the complex environment of an operational cell without contaminating the system. The novelty of this work is that while liquid-phase PIV measurements in microchannels have been widely demonstrated [11–13], gas-phase PIV measurements in microchannels (or mm-scale channels) are yet nascent.

Since PIV is based on imaging of particulates introduced into the flow, the accuracy of the gas-phase flow velocity measurement is strongly dependent on the ability of the particle to follow the flow. In the current work, water droplets have been used as seed particles for measuring the flow in a straight channel. But, certain limitations are encountered when trying to use water droplets as seed particles in flows with significant decelerations, such as the flow in a 180° switchback with 1:1 channel to land ratio. The Stokes number provides a measure of the particles' ability to accurately track the flowfield, and the limiting Stokes number also depends on the flow geometry and the presence of significant accelerations or decelerations. In order to assess the ability of the particles to track the flowfield, a series of numerical fluid velocity and particle trajectory simulations have been performed in a 180° switchback flow geometry for Reynolds numbers of 50–400. As expected, the fluid velocity field contains regions of separation and recirculation near the sharp corners. Next, numerical simulations of water particle trajectories as a function of water droplet diameter (1–5 μm) were performed. By comparing the present simulations of the water particle trajectories and of the flow velocity, limiting conditions for the fidelity of the measurement are identified.

2. Experimental set-up

Fig. 1(a) shows a schematic of the flow delivery system and temperature controls. The flow rate of dry, compressed air was controlled using a digital flow meter and a flow control valve. The flow delivery system has two possible paths for the air flow depending upon whether the desired seeding is smoke particles or water droplets. Either a smoke generator or a mist (water droplet) generator was included in the flow loop, as appropriate. The flow could be heated to reproduce conditions similar to that in an operational cell. Tubing and channel wall temperatures were controlled to within ±1 °C by PID controllers. Air temperatures of both 60 °C and 80 °C were employed and the relative humidity was near 100%.

Fig. 1(b) shows a schematic illustration of the PIV system setup. The measurement system consisted of 12-bit CCD camera with 2 K pixel × 2 K pixel resolution, an Olympus research microscope with 5× objective lens, dual-pulse Nd-Yag laser, a synchronizer and the image capture board/software. A 50-μm thick light sheet was projected into the side of the channel.

The basic principle of particle image velocimetry (PIV) is that two laser-illuminated images of the (seeded) flow are acquired at successive time instants, separated by Δt. The seed particles, illuminated by the laser, appear as bright spots in the digital image. Each image is broken down into a series of interrogation windows, typically 64 pixels × 64 pixels, although

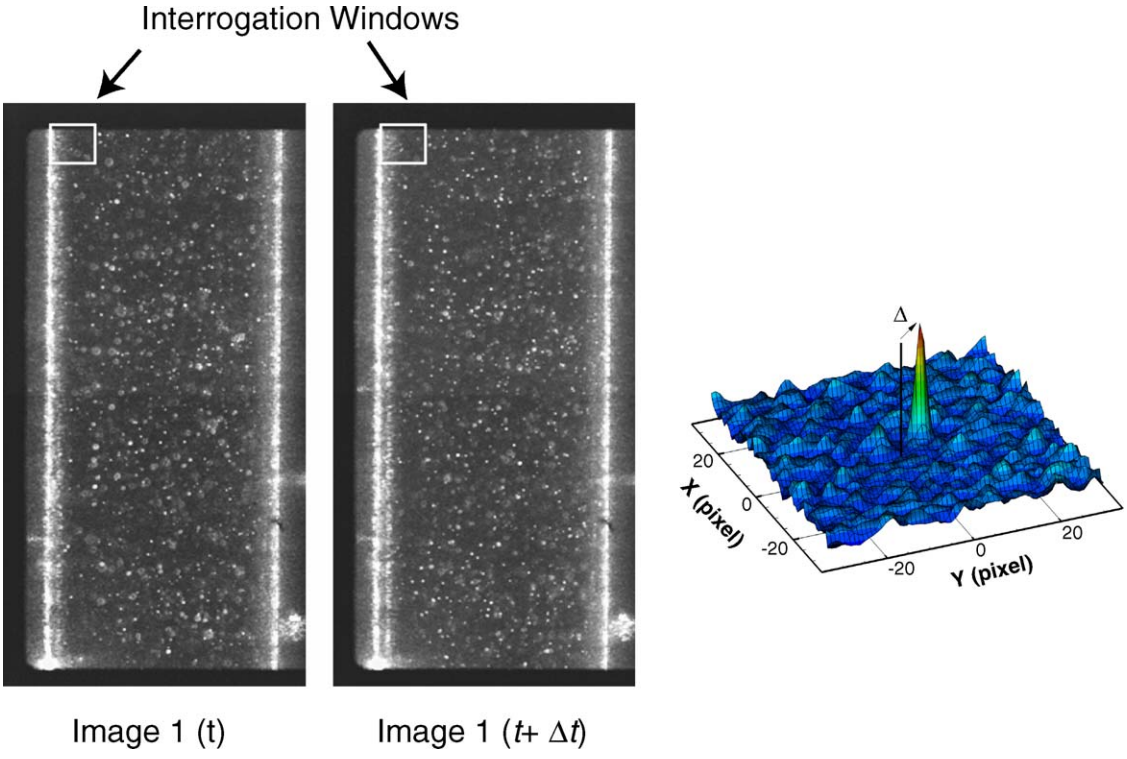

Fig. 2. Typical images separated by Δt, plus representative interrogation windows and cross-correlation function for interrogation windows in image 1 and image 2. Δ in the cross-correlation plot gives the average displacement of the image intensities between images and when divided by Δt, provides a quantitative velocity vector centered at the center of the interrogation window.

smaller/larger or rectangular interrogation windows can be used as needed. An example of two images, interrogation windows, and a representative cross-correlation signal is shown in Fig. 2. For each interrogation window, the intensity of the signal within the window is cross-correlated between image 1(t) and image 2($t + \Delta t$). The cross-correlation peak within this window corresponds to an average displacement of the seed particles (Δ), and when divided by Δt, provides an average velocity for the particles within this interrogation window. A velocity field can be built up by cross-correlating the full series of interrogation windows within an image pair. The spatial resolution is typically defined as the distance between centers of the interrogation windows. Further background on the general PIV technique can be found in Adrian [14] and Raffel et al. [15].

In the present study, measurements were made in a 1-mm wide straight acrylic channel, in a 1-mm wide polydimethylsiloxane (PDMS) channel with integrated heater, and in a PDMS 180° switchback flow model. When water droplets are used as seed in a heated flow, the actual channel must also be heated in order to prevent image-obscuring condensation from occurring on the top surface. The PDMS flow channel model with integrated heater and fabrication process is shown in Fig. 3.

As discussed previously, a key challenge that must be surmounted in order to make gas flow PIV measurements in a confined channel of millimeter scale or smaller is the identification and generation of appropriate seed particles. The issue is further complicated if one wishes to identify a seeding technique that may be extended to use in situ in operational cells, since the seed particles must not contaminate the system. In the present work, the smoke particles were generated by slow-burning smoke coils, and had particle diameters estimated at less than 1 μm. An ultrasonic mist generator was used to generate the water droplet particles, with diameters of approximately 1–8 μm [16]. Both of these seed particle generators were mounted in-line with the flow delivery system. In the case of the water droplets, the seeding density was observed to decrease with increasing temperature [17], however, even at a typical operating temperature of 80 °C, the seeding density was sufficient for obtaining the velocity field data presented herein.

In the present experimental setup, the model flow channel is optically accessible both from the top and the side. Since

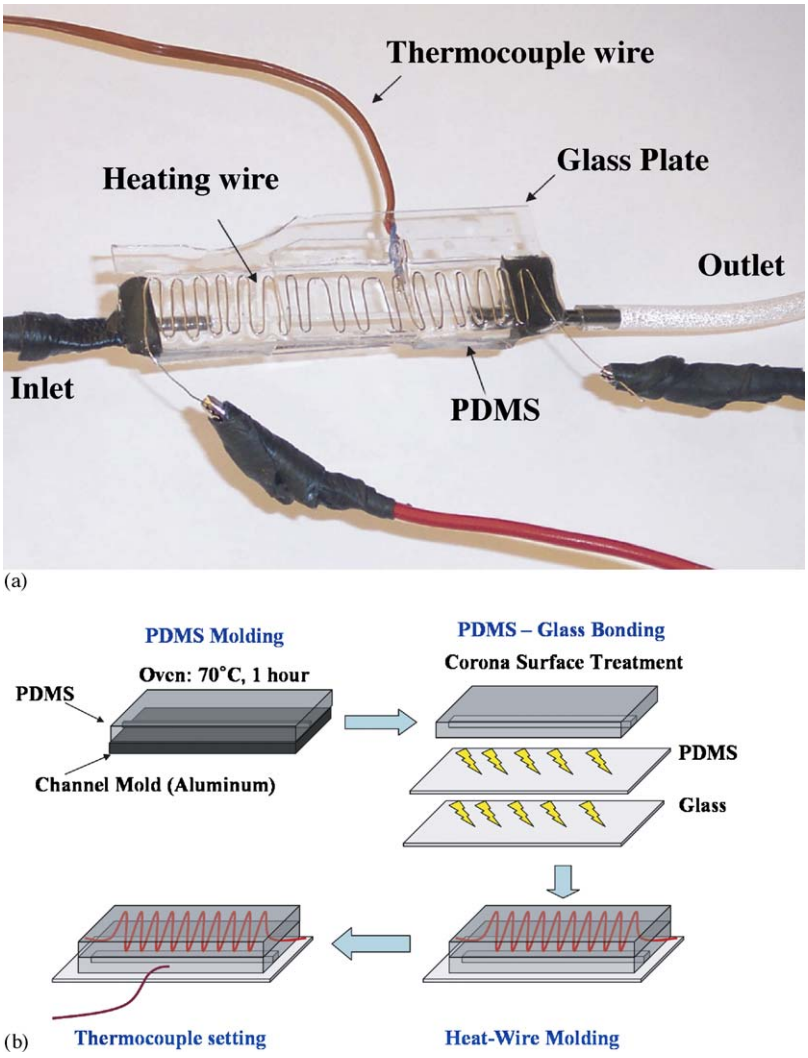

Fig. 3. (a) PDMS model flow channel with integrated heater. (b) Fabrication process of the PDMS channel.

the laser sheet is projected through the side of the channel, such optical access is critical to the measurement of the velocity field. In order to extend the technique to in situ applications, specially designed optically accessible cells would be required.

3. Results and discussion

In order to test the feasibility of using smoke particles as seed particles, measurements of gas velocities in a straight channel with 1 mm width × 1 mm height were acquired. The Reynolds number of the flow was 70, which represents the low end of realistic Reynolds numbers in the gas flow reactant channels of an operational fuel cell.

Fig. 4 shows the ensemble-averaged velocity field calculated from smoke particle image pairs and the velocity profile extracted from the ensemble-averaged vector fields. The ensemble included 50 instantaneous measurements of the laminar flow. The interrogation window size was 128 pixels × 128 pixels, and 50% overlapping was allowed. The entrance length, L_e, was estimated to be approximately 2.1 mm based on laminar flow theory [18], and the measurement area was over 10 mm downstream of the inlet. The velocity profile is in good agreement with the parabolic Poiseuille profile as shown in Fig. 4.

An air flow velocity field in a 180° switchback was measured with a similar PIV setup, again using smoke particles for flow seeding. Fig. 5(a) shows the geometry of the test section, and the channel had a height of 1 mm (into the page). The Reynolds number was 700, where the Reynolds number was selected to replicate the flow in a typical operational cell. The interrogation window size was 64 pixels × 64 pixels and a 50% overlapping of windows was used in the analysis. Fig. 5(b) shows the ensemble-averaged velocity field in the 180° switchback. The spatial resolution of this measurement is 42 μm in x and y. Recirculation and separation regions can be observed in the 180° switchback. Because the size of the recirculation region is relatively large as compared to the channel area, this recirculation

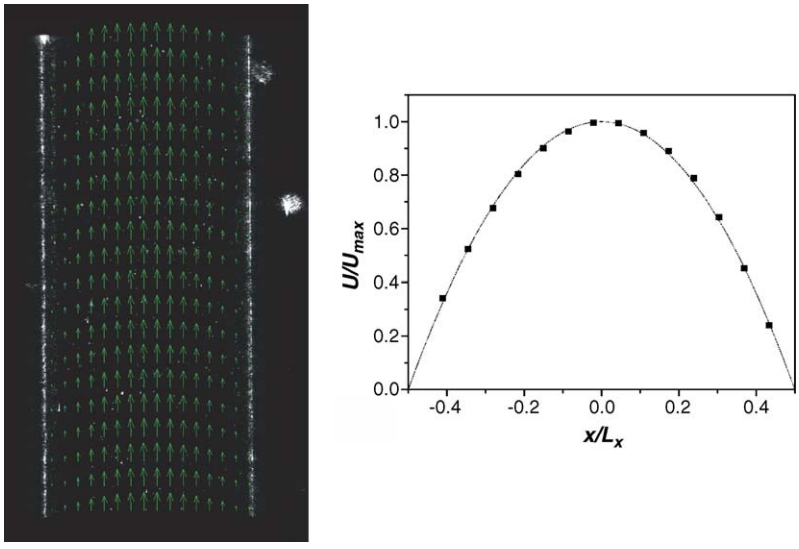

Fig. 4. Ensemble-averaged velocity field data calculated from smoke particle images and velocity profile. Points represent the PIV data and the dashed line represents the theoretical parabolic Poiseuille profile.

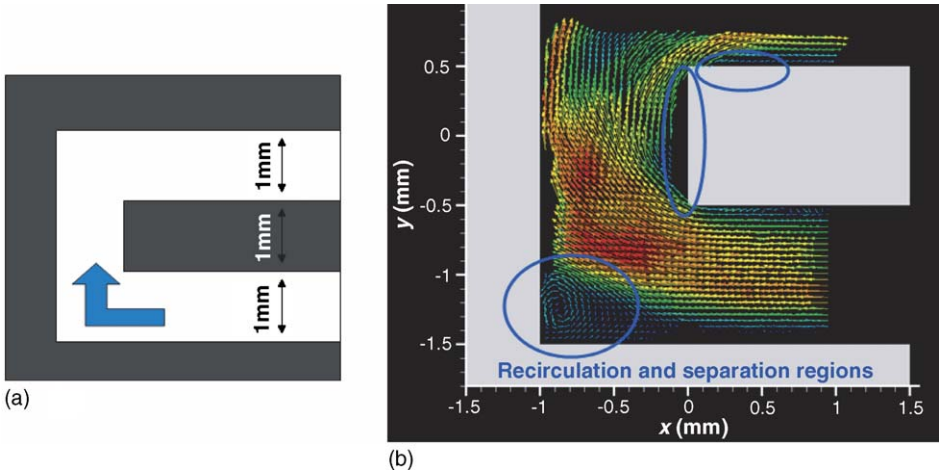

Fig. 5. (a) Geometry of 180° switchback flow. (b) Measured velocity in the 180° switchback. The spatial resolution of this measurement is 42 μm in x and 42 μm in y.

region might cause unexpected effects in an operational cell, e.g. increased parasitic load, reduced performance with local flooding, and accumulation of liquid water storage in the diffusion media and channels as observed with neutron imaging [19].

The second part of this study aims to develop an appropriate seed technique for use in an operational cell, and involved seeding a heated and humidified air flow with water particles. In the experiment, the relative humidity and temperature of the flow are typical of those encountered in an operational cell. Water particles with a size distribution of approximately 1–8 μm [16] were injected into the gas phase fluid (in this case, air) and PIV measurements were acquired. As previously mentioned, given the humidity and temperature of the flow, the channel was heated to both 60 °C and 80 °C (in separate experiments) to simulate a true fuel cell environment and to prevent condensation on the optical surfaces. Fig. 6 shows an image and averaged velocity fields using water droplet seeding in a non-operational flow channel model. The spatial resolution of this measurement is 42 μm in x and 63 μm in y. This measurement was acquired at approximately 10 mm downstream of the channel entrance. Since the entrance length of the channel is estimated at approximately 20 mm [18], the velocity profiles are not expected to be fully developed. Developing flow results in a greater pressure drop through the channels than predicted with the simplified fully developed flow equations commonly used. The primary result of interest in Fig. 6 is that this seed technique shows significant potential for application to the acquisition of velocity measurements in operational cell conditions (temperature, humidity) without introducing a contaminating substance.

Tests were performed to assess the usefulness of using water droplets as seed particles for PIV studies of corner flows. It was readily determined that water droplets with the current size distribution are unable to respond to the rapid flow decelerations present in some corner flows.

The Stokes number is defined as:

$$St = \frac{\rho_p d_p^2 U C_c}{18 \mu L} \tag{1}$$

where ρ_p is particle density, d_p particle diameter, U a characteristic velocity scale of the flow, C_c a slip correction factor [20], μ the fluid viscosity, and L a characteristic length scale of the flow. The Stokes number, St, is a measure of particle inertia and represents the ratio of the particle response time to characteristic flow timescale [21]. As $St \to 0$, the particles and fluid trajectories are equivalent. For high fidelity of the fluid velocity measurement, it is desirable to have a very low Stokes number. In a practical application of the measurement technique, the flow geometry, flow conditions (including Reynolds number), and fluid are typically defined by the problem of interest. It is thus left to the investigator to select seed particles with characteristics (particle density and average diameter) that allow for the Stokes number to be minimized. We are interested in identifying the limiting Stokes number condition. To that end, we have performed a series of fluid velocity and particle trajectory numerical simulations to identify the maximum diameter of water particles

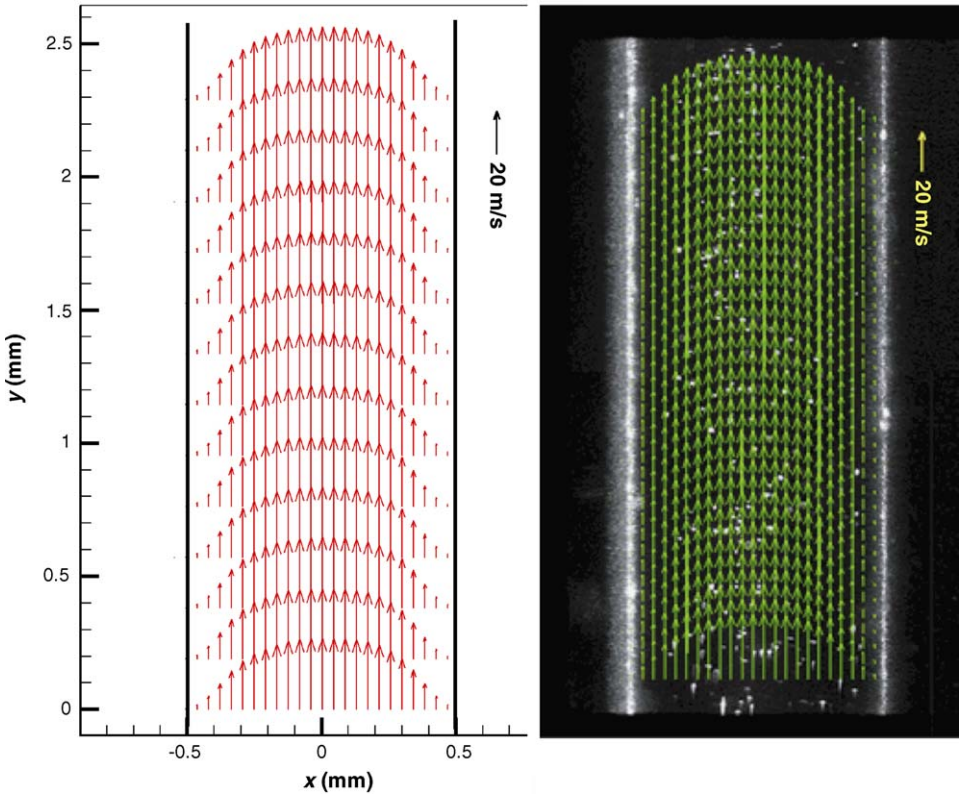

Fig. 6. Measurement of the velocity field of an airflow in a 1-mm wide channel with Reynolds number of 820, where water droplets were used as the seed particles. The spatial resolution of this measurement is 42 μm in x and 63 μm in y.

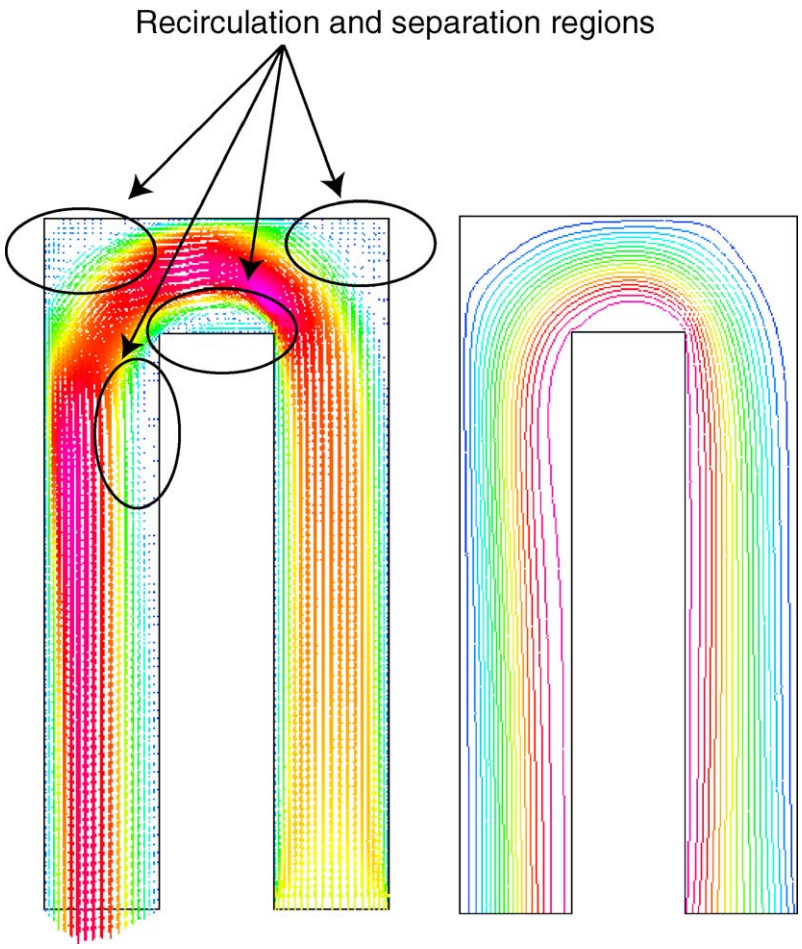

Fig. 7. Numerical simulation of the fluid velocity vector field and streamlines in a 180° switchback flow with Reynolds number of 400.

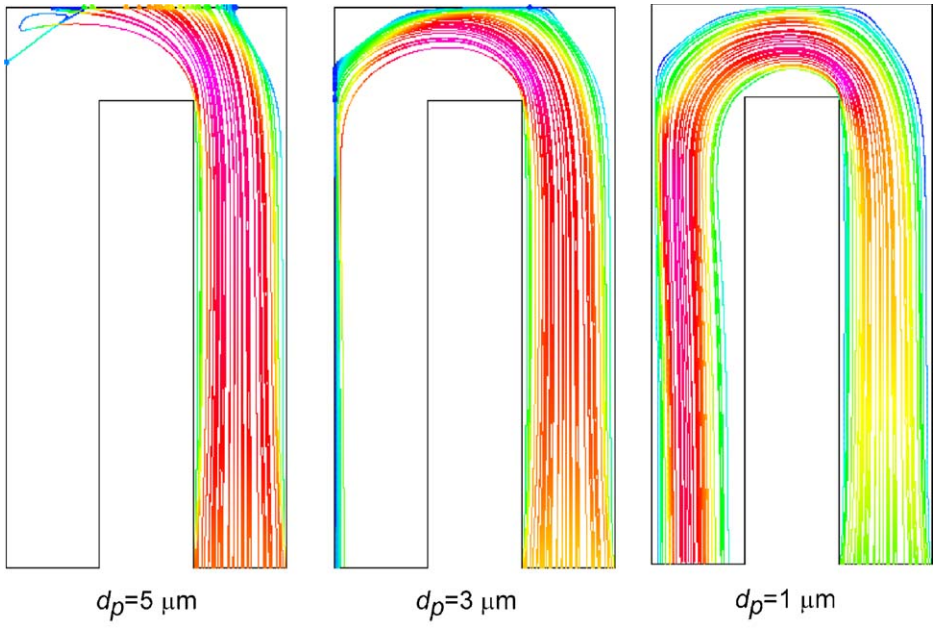

Fig. 8. Numerical simulation of water droplet trajectories as a function of diameter in a 180° switchback flow with Reynolds number of 400.

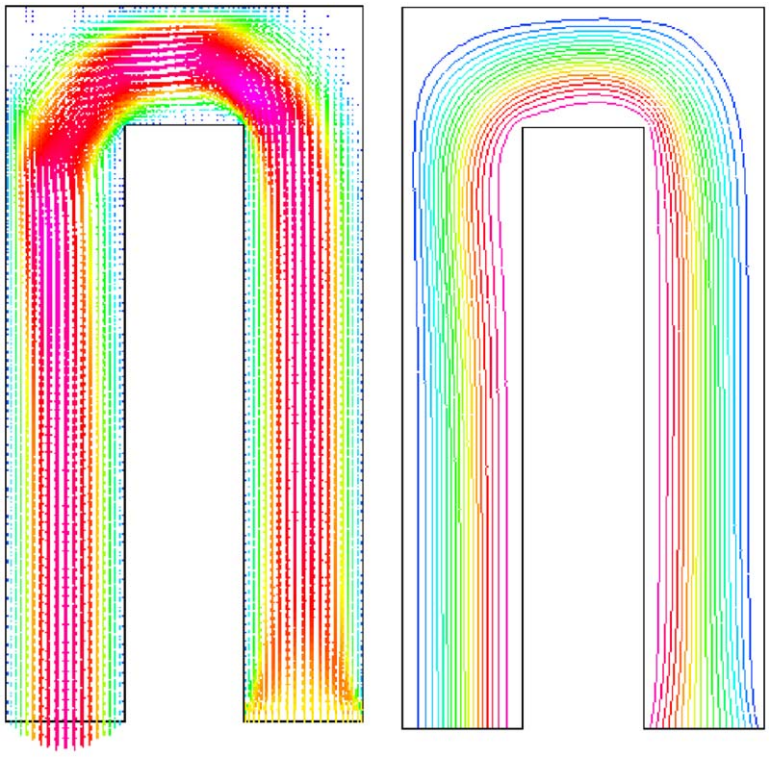

Fig. 9. Numerical simulation of the fluid velocity vector field and streamlines in a 180° switchback flow with Reynolds number of 50.

allowable for one to obtain a reasonable representation of fluid velocity from this measurement technique in the specific case of gas flow in a 180° switchback for Reynolds numbers ranging from 50 to 400. Fig. 7 shows a numerical simulation of the velocity field in a 180° switchback flow for Reynolds number of 400. Numerical simulations of water particle trajectories as a function of diameter in the same geometry are shown in Fig. 8. The conclusion that can be drawn from these simulations is that, in order for the water particle trajectories to accurately represent the flow dynamics in this geometry and for a Reynolds number of 400, the water particles must have a diameter of approximately 1 μm. While the ability of the particles to track the flow as a function of diameter can be assessed from a comparison of the particle trajectory simulations and the fluid velocity simulations, the conclusion that 1 μm particles are significantly more capable of responding to the flow could also be made on the basis of the calculation of Stokes number for the same physical conditions ($Re = 400$, $L = 1$ mm, $T = 60\,^{\circ}$C). For example, using a slip cor-

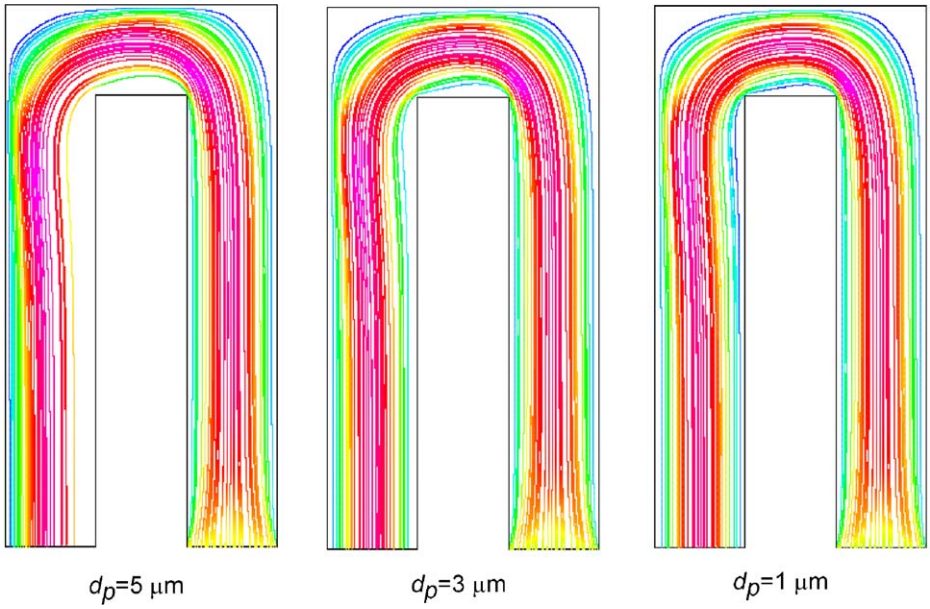

Fig. 10. Numerical simulation of water droplet trajectories as a function of diameter in a 180° switchback flow with Reynolds number of 50.

rection factor, C_c, of 1.033 for 5 μm particles and 1.17 for 1 μm particles [20], the Stokes number is 0.53 for 5 μm water particles and 0.02 for 1 μm water particles. So quantitatively, the 1 μm particles would give $St \ll 1$, as desired. If the water particles are larger than 1 μm, they are unable to respond to the deceleration and instead many of them impinge upon the outside corner of the channel, as was observed in an actual experiment. For a flow in the same geometry with Reynolds number of 50, the decelerations are not as severe, and the required particle diameter is slightly higher, as can be determined from comparing the numerical fluid velocity simulations (Fig. 9) and the numerical particle trajectory simulations (Fig. 10). Once a technique is identified for generating water droplets with diameters of less than 1 μm, it is expected that water droplet-based PIV may be applied to the 180° switchback or other relevant flow geometries. Recent research into the generation of water droplets with diameter of 1 μm or less suggests that such droplets may be obtainable in the near future [22,23].

4. Summary and conclusions

Gas-phase PIV has been demonstrated in channels with characteristic dimension of 1–2 mm with a particular emphasis on conditions suitable for development of fuel cell reactant flow channels. PIV data were acquired in these millimeter-scale channels using both smoke particles and water droplets to seed the air flow, and at temperatures and Reynolds numbers similar to those in an operational cell. The spatial resolution of these measurements is 40–60 μm, depending on the experimental setup, an improvement of approximately 5–10 times the resolution of that cited in Martin et al. [3]. The use of water droplets as seed particles is the most promising for application to in situ measurements in operational fuel cells since the addition of water droplets will not contaminate the complex system. However, based upon both experimental and numerical results, particles smaller than 1 μm are required in order to accurately follow the flow in regions of rapid deceleration. The seeding, acquisition and analysis techniques used in obtaining these will serve as a basis for ongoing development of diagnostic techniques for measurements of the gas-phase velocity in situ in an operational cell.

References

[1] J. Larminie, A. Dicks, Fuel Cell Systems Explained, Wiley & Sons, West Sussex, England, 2003, pp. 94–96.
[2] D.P. Wilkinson, O. Vanderleeden, Handbook of Fuel Cells, in: W. Vielstich, A. Lamm, H.A. Gasteiger (Eds.), Fundamentals, Technology and Applications, 3, John Wiley & Sons, New York, 2003, p. 315.
[3] J. Martin, P. Oshkai, N. Djilali, J. Fuel Cell Sci. Tech. 2 (2005) 70–80.
[4] M. Hickner, K. Chen, Paper #FUELCELL2005-74118, in: Proceedings of the FUELCELL2005 Third International Conference on Fuel Cell Science Engineering & Technology, Ypsilanti, MI, 2005.
[5] K. Tüber, D. Pócza, C. Hebling, J. Power Sources 124 (2003) 403–414.
[6] X.G. Yang, F.Y. Zhang, A.L. Lubawy, C.Y. Wang, Electrochem. Solid-State Lett. 7 (2004) A408–A411.
[7] H. Yang, T.S. Zhao, Q. Ye, J. Power Sources 139 (2005) 79–90.
[8] H. Yang, T.S. Zhao, P. Cheng, Int. J. Heat Mass Trsfr. 47 (2004) 5725–5739.
[9] H.S. Kim, T.H. Ha, S.J. Park, K. Min, M.S. Kim, Paper #FUELCELL2005-74113, in: Proceedings of the FUELCELL2005 Third International Conference on Fuel Cell Science Engineering & Technology, Ypsilanti, MI, 2005.
[10] B. Ladewig, R. Blewitt, J. Shrimpton, A. Kucernak (2004) unpublished.
[11] C.D. Meinhart, S.T. Wereley, J.G. Santiago, Exp. Fluids 27 (1998) 414–419.
[12] J.G. Santiago, S.T. Wereley, C.D. Meinhart, D.J. Beebe, R.J. Adrian, Exp. Fluids 25 (1998) 316–319.
[13] D. Sinton, Microfluid. Nanofluid. 1 (2004) 2–21.
[14] R.J. Adrian, Annu. Rev. Fluid Mech. 23 (1991) 261–304.
[15] M. Raffel, C. Willert, J. Kompenhans, Particle Image Velocimetry: A Practical Guide, Springer-Verlag, Berlin, 1998.
[16] A. Lozano, H. Amaveda, F. Barreras, X. Jordà, M. Lozano, J. Fluids Eng. 125 (2003) 941–945.
[17] S.Y. Yoon, J.W. Ross, K.V. Sharp, Proceedings of 6th International Symposium on Particle Image Velocimetry (PIV05), Pasadena, CA, 2005.
[18] F.M. White, Fluid Mechanics, fifth ed., McGraw Hill, New York, 2003, pp. 348–351.
[19] N. Pekula, K. Heller, P.A. Chuang, A. Turhan, M.M. Mench, J.S. Brenizer, K. Ünlü, Nuc. Inst. Meth. Phys. Res. Section A: Accel., Spectrom., Detect. Assoc. Equip. 542 (2005) 134–141.
[20] W.C. Hinds, Aerosol Technology, John Wiley and Sons, New York, 1982, pp. 44–47, 407–408.
[21] W.C. Hinds, Aerosol Technology, John Wiley and Sons, New York, 1982, pp. 104–124.
[22] S. Ter-Avetisyan, M. Schnürer, H. Stiel, P. Nickles, J. Phys. D: Appl. Phys. 36 (2003) 2421–2426.
[23] L.C. Mountford, R.A. Smith, M.H.R. Hutchinson, Rev. Sci. Instr. 69 (1998) 3780–3788.